

Exome capture sequencing identifies a novel mutation in *BBS4*

Hui Wang,^{1,2} Xianfeng Chen,² Lynn Dudinsky,⁹ Claire Patenia,¹ Yiyun Chen,² Yumei Li,^{1,2} Yue Wei,¹⁰ Emad B. Abboud,¹¹ Ali A. Al-Rajhi,¹¹ Richard Alan Lewis,^{2,3,4} James R. Lupski,^{2,4,5} Graeme Mardon,^{2,5,6,7,8} Richard A. Gibbs,^{1,2} Brian D. Perkins,⁹ Rui Chen^{1,2,8}

¹Human Genome Sequencing Center, Baylor College of Medicine, Houston, TX; ²Department of Molecular and Human Genetics, Baylor College of Medicine, Houston, TX; ³Department of Ophthalmology, Baylor College of Medicine, Houston, TX; ⁴Texas Children's Hospital, Baylor College of Medicine, Houston, TX; ⁵Department of Neurology, Baylor College of Medicine, Houston, TX; ⁶Department of Neuroscience, Baylor College of Medicine, Houston, TX; ⁷Department of Pathology, Baylor College of Medicine, Houston, TX; ⁸Program in Developmental Biology, Baylor College of Medicine, Houston, TX; ⁹Department of Biology, Texas A&M University, College Station, TX; ¹⁰Leukemia Department, University of Texas, M. D. Anderson Cancer Center, Houston, TX; ¹¹King Khaled Eye Specialist Hospital, Riyadh, Kingdom of Saudi Arabia

Purpose: Leber congenital amaurosis (LCA) is one of the most severe eye dystrophies characterized by severe vision loss at an early stage and accounts for approximately 5% of all retinal dystrophies. The purpose of this study was to identify a novel LCA disease allele or gene and to develop an approach combining genetic mapping with whole exome sequencing.

Methods: Three patients from King Khaled Eye Specialist Hospital (KKESH205) underwent whole genome single nucleotide polymorphism genotyping, and a single candidate region was identified. Taking advantage of next-generation high-throughput DNA sequencing technologies, whole exome capture sequencing was performed on patient KKESH205#7. Sanger direct sequencing was used during the validation step. The zebrafish model was used to examine the function of the mutant allele.

Results: A novel missense mutation in Bardet-Biedl syndrome 4 protein (*BBS4*) was identified in a consanguineous family from Saudi Arabia. This missense mutation in the fifth exon (c.253G>C;p.E85Q) of *BBS4* is likely a disease-causing mutation as it segregates with the disease. The mutation is not found in the single nucleotide polymorphism (SNP) database, the 1000 Genomes Project, or matching normal controls. Functional analysis of this mutation in zebrafish indicates that the G253C allele is pathogenic. Coinjection of the G253C allele cannot rescue the mislocalization of rhodopsin in the retina when *BBS4* is knocked down by morpholino injection. Immunofluorescence analysis in cell culture shows that this missense mutation in *BBS4* does not cause obvious defects in protein expression or pericentriolar localization.

Conclusions: This mutation likely mainly reduces or abolishes *BBS4* function in the retina. Further studies of this allele will provide important insights concerning the pleiotropic nature of *BBS4* function.

The molecular mechanisms underlying genetic diseases are often highly heterogeneous. Specifically, mutations in different genes can result in the same clinical phenotype. In addition, patients with different mutations, or even the same mutation, in one gene can manifest different clinical phenotypes. This underscores the importance of comprehensive documentation of phenotype and genotype relationships as the first step in accurate and personalized treatment of the disease. Leber congenital amaurosis (LCA; OMIM 204000) most often presents as a recessive disease, is one of the most severe forms of vision loss, is apparent by 1 year of age, and accounts for more than 5% of all retinal dystrophies [1,2]. The clinical features of this genetically heterogeneous disease include severe and early visual loss, sensory nystagmus, amaurotic pupils, and absent electrical signals on electroretinogram (ERG) [1,3]. To date, at least 15 genes have been associated with LCA, and they act in

strikingly diverse genetic and functional pathways, including retina development, phototransduction, vitamin A metabolism, protein transport, and centrosome formation [4-11]. As a result, accurate molecular diagnosis of the disease is essential for developing and providing proper treatment to the patient. Indeed, gene and drug therapy have recently been developed specifically for patients with mutations in retinal pigment epithelium 65 (*RPE65*) [12,13].

Despite the substantial efforts in human mapping studies during the last decade, about 35% of LCA familial cases in the European population cannot be accounted for by mutations in the 15 known LCA genes. The portion of LCA patients with unknown mutations in other populations may be significantly higher [7,14]. These cases can be partially explained by novel LCA disease genes. Gene identification becomes increasingly difficult as each likely accounts for only a small fraction of the patients with this rare disease. Some of these patients may carry mutations in other known retinal disease genes not been previously linked to LCA. This is particularly likely for genes normally associated with syndromic retinal degenerative diseases. Indeed, researchers

Correspondence to: Rui Chen, Department of Molecular and Human Genetics, Baylor College of Medicine, Houston, TX; Phone: (713) 798-5194; Fax: (713) 798-5741; email: ruichen@bcm.edu

have reported that several syndromic diseases, such as Alström syndrome, Batten disease, Joubert syndrome (JBTS), peroxisomal diseases, and Senior-Loken syndrome (SLSN), show an “LCA-like ocular phenotype” [6]. The mutations in some known LCA disease genes can also cause syndromic diseases. For example, Centrosomal protein of 290 kDa (*CEP290*, also known as *NPHP6*), which represents the most common cause of LCA identified to date [15,16], is also associated with other diseases, such as retinitis pigmentosa [17], Meckel syndrome (MKS) [18,19], SLSN [20], Bardet-Biedl syndrome (BBS) [21] and JBTS [22,23]. Similarly, Bardet-Biedl syndrome protein-8 (*BBS8*), one of the genes involved in BBS, has been linked to retinitis pigmentosa [24].

Since more than 165 genes have been associated with retinal diseases ([RetNet](#)), screening for mutations in all of these genes with traditional Sanger sequencing is cost prohibitive. The recent development of next-generation sequencing technology provides a much faster and more cost-effective alternate approach for identifying causative mutations [25-28]. For example, the entire exome of an individual can be sequenced at great depth with a single lane of the Illumina HiSeq 2000 sequencer coupled with DNA capture technology [29-32]. Indeed, several disease-causing mutations have been identified with exome sequencing of a small number of patients, underscoring the great potential of this technology [33-41].

To test the feasibility of identifying disease-causing mutations with direct sequencing, we employed a combination of genetic mapping and the whole exome sequencing approach. Based on single nucleotide polymorphism (SNP) mapping, we first mapped the disease locus of a Saudi family to an 11.2 Mb region on chromosome 15. With whole exome capture and sequencing, we identified a missense mutation in *BBS4* ([NM_033028](#)), one of the 14 genes known to cause BBS ([OMIM 209900](#)) [42]. This mutation was further confirmed with Sanger sequencing and family segregation. *Bbs4* zebrafish was used to determine the functional relevance of this allele. In contrast, the mutant *BBS4* mRNA with the missense allele cannot rescue the gastrulation and the retinal phenotype, while the wild-type human *BBS4* mRNA can successfully rescue the gastrulation and the retinal phenotype. Our results are the first report that links *BBS4* with LCA and indicates that partial loss of *BBS4* function can cause an LCA-like phenotype with quite mild syndromic features.

METHODS

Subjects: The study was approved by the Human Subjects Ethics Subcommittee of Baylor College of Medicine. We obtained blood samples and pedigrees after receiving informed consent from all individuals. Approval was obtained from the institutional review boards of the participating centers. Family KKESH205 was recruited by Dr. Lewis

through the King Khaled Eye Specialist Hospital (KKESH) in Riyadh, Saudi Arabia. Blood samples from all available family members were collected and processed at KKESH hospital in Riyadh, Saudi Arabia with the Qiagen (Germantown, MD) blood genomic DNA extraction kit following the protocol provided by the manufacturer.

Whole exome capture and library construction: Five µg of genomic DNA from KKESH205#7 was used to make a SOLiD fragment library. After the SOLiD adaptors were ligated to the genomic DNA, five cycles of PCR amplification were applied. This DNA was then hybridized to oligonucleotides from NimbleGen’s (Madison, WI) liquid capture kit (the Consensus CDS design design) for 72 h to enrich exonic regions. Hybridized fragments were eluted and sequenced with single end 50 bp reads on a SOLiD platform.

Sanger sequencing: Primers surrounding the variant were designed with the online program Primer3, and PCR products were purified with ExoSAP-IT (USB Corp, Cleveland, OH). Sequencing chemistry was performed using an ABI (Life Technology, Carlsbad, CA) PRISM Big Dye Terminator Cycle Sequencing Ready Reaction Kit (v3.1), the PCR amplicon sequenced on an ABI 3700, and the results analyzed using Sequencher software.

Morpholino knockdown: Wild-type zebrafish of an AB/Ekkwill hybrid strain were housed, bred, and staged according to standard procedures [43]. Wild-type embryos (n=280–300) were injected at the 1–2 cell stage with 4.0 ng of a *bbs4* morpholino (GeneTools, Philomath, OR) designed to block translation of *bbs4* mRNA (5'-GAA AAA GAT CAC TAC TGT AAA GCA T-3'). To quantify our results, we used a classification scheme similar to one previously described [44]. Embryos with normal somites and notochord but a shortened body axis were considered mild, whereas embryos with broad, flattened somites and severely kinked notochords were considered severe.

Immunohistochemistry: Larvae were fixed in 4% paraformaldehyde in PBS (137 mM NaCl, 10 mM phosphate, 2.7 mM KCl, pH 7.4) for 2–4 h at 4 °C. Following fixation, samples were washed in PBST (PBS + 0.01% Tween-20) and equilibrated with 30% sucrose/PBS at 4 °C. Samples were oriented in 100% Tissue-Tek OCT (Miles, Inc., Elkhart, IN) and frozen at –20 °C. Cryosections (10 µm thick) were mounted on gelatin-coated slides, and dried for 2–3 h at room temperature. Slide edges were lined with a hydrophobic marker (PAP pen) and washed with PBS before blocking for 1 h (PBS + 0.05% Tween-20 + 0.1% dimethyl sulfoxide + 0.1% BSA). The 1D1 antibody (gift of Dr. James Fadool, Florida State University, Tallahassee, FL) was diluted 1:100 in blocking solution and incubated overnight at 4 °C in a humid chamber. Slides were washed with PBST before incubation with the appropriate fluorescent-conjugated secondary antibodies. Slides were counterstained with 4',6-diamidino-2-phenylindole (DAPI; Invitrogen, Carlsbad, CA)

to label DNA. Slides were washed 3× for 10 min in PBST, and coverslips were mounted with Vectashield (Invitrogen). Images were obtained using a Zeiss AxioImager (Zeiss, Thornwood, NY) compound microscope with an ApoTome attached.

RNA synthesis: The wild-type and mutant *BBS4* alleles were amplified with PCR and cloned into pBluescript (Fermentas, Inc., Glen Burnie, MD). The plasmids were linearized with BamHI, purified, and used as a template for in vitro transcription to generate 5'-capped mRNAs with the mMESSAGE mMACHINE kit (Ambion, Austin, TX). Synthetic mRNA (150–300 pg) was injected alone or coinjected with morpholinos.

In situ hybridization: Digoxigenin-labeled antisense riboprobes were synthesized from full-length cDNAs using standard protocols. The *pax2.1* and *myoD* full length cDNAs were gifts from Dr. Arne Lekven (Texas A&M University, College Station, TX). In situ hybridizations were performed as previously described [45].

Cell transfection: HeLa cells were transfected with 1 µg of *pCmv-BBS4* cDNA and used for immunostaining 24 h later. HeLa cells were fixed with methanol/acetone (1:1) at room temperature for 10 min and blocked with PBS-10% fetal bovine serum (FBS) for 10 min before primary antibody was added. Primary antibodies (mouse anti-FLAG 1:100 and rabbit anti-gamma-tubulin, Sigma, St. Louis, MO) in PBS-5% FBS were incubated with the cells at 37 °C for 2 h, followed by washing. The cells were incubated with secondary antibodies (Annexin V-antimouse, Cy3-antirabbit) in PBS-5% FBS (1:1,000) at 37 °C for 1 h. The cells were washed, DAPI stained, and mounted.

Bioinformatic analyses: To analyze the large amount of exome sequencing data, a semiautomated pipeline was constructed to identify putative disease-causing mutations. First, all reads were mapped to the human reference genome (NCBI build 36) using BWA (Ver. 0.5.0) with default parameters [46]. Reads that mapped to multiple positions in the genome were excluded from further analysis. Second, putative variants, including single nucleotide variants or insertions or deletions (in/dels), were identified using Samtools [47]. A cutoff score of 40 or variance bases at both strands with a confidence score greater than 30 were used to exclude low-quality variants. Furthermore, only variants with allele frequencies greater than 15% were kept.

RESULTS

Clinical features: KKESH205 is a consanguineous Saudi Arabian family. Within the family, there are three affected and four unaffected members (Figure 1A). All affected members of KKESH205 show typical LCA phenotypes, including lack of ERG, infantile nystagmus, and pigmentary retinopathy with a “rubelliform” appearance. In addition, several mild phenotypes have been observed, including delayed walking

(after age 2), slowness in learning speech (after age 3 and 4), and mild facial dysmorphism with bilateral enophthalmos.

Homozygosity mapping: To identify the causative mutation in this family, we first performed direct Sanger sequencing to check all the coding exons from all 15 known LCA disease genes in one affected member of KKESH205. No homozygous mutations were identified within the coding regions of these 15 genes (data not shown). Therefore, homozygosity mapping of the disease locus was performed by genotyping all three affected members of KKESH205 using the Illumina 370K SNP array. A single 11.2 Mb homozygous region on chromosome 15 is shared by all three affected members, and therefore it almost certainly contains the disease locus (Figure 1B). Consistent with the Sanger sequencing described above, this region contains no known LCA disease genes. Due to the high gene density in this region, direct Sanger sequencing of all coding exons in this 11.2 Mb span was prohibitively expensive and labor intensive.

Mutation detection: Since the development of a custom designed regional capture is time-consuming and costly, we decided to apply whole-exome capture sequencing to one affected individual (KKESH205#7) while focusing the analysis on the candidate region to identify the disease-causing mutation in this family. A total of about 1.6 million reads uniquely map to the exons with an average of 18.6X coverage. Moreover, 93% of targeted exons have at least 1X coverage (Figure 2). Based on the filtering criteria (see Methods), a total of 370,000 SNPs and in/dels were identified for further analysis. Since disease-causing variants for LCA should be rare in the human population, common variants were filtered out. Variants found in the Single Nucleotide Polymorphism database ([dbSNP database](#)) or the 1000 Genomes SNP database at frequency greater than 0.5% were excluded, and the remaining variants are likely to be rare. As expected, most variants (96.4%) identified in this individual are indeed common. Finally, variants that did not lead to coding changes (i.e., synonymous) were excluded. Based on the current reference gene annotation, only variants that affect protein coding changes or splicing were subject to downstream analysis. As a result, 352 candidate variants, all of which are single nucleotide changes, were identified in the entire exome ([Appendix 1](#)).

As described previously, homozygous mapping of this consanguineous KKESH205 family via high-density SNP genotyping arrays identified a single critical region on chromosome 15. Inspection of the 352 candidate variants revealed only one homozygous missense change in this locus. This missense mutation (G-C) is located in the fifth exon of *BBS4*, a gene known to cause BBS, a rare human genetic disorder characterized by obesity, retinal dystrophy, renal anomalies, hypogenitalism, polydactyly, and numerous developmental and behavioral defects [48]. As ocular phenotypes are a common clinical feature of BBS and LCA,

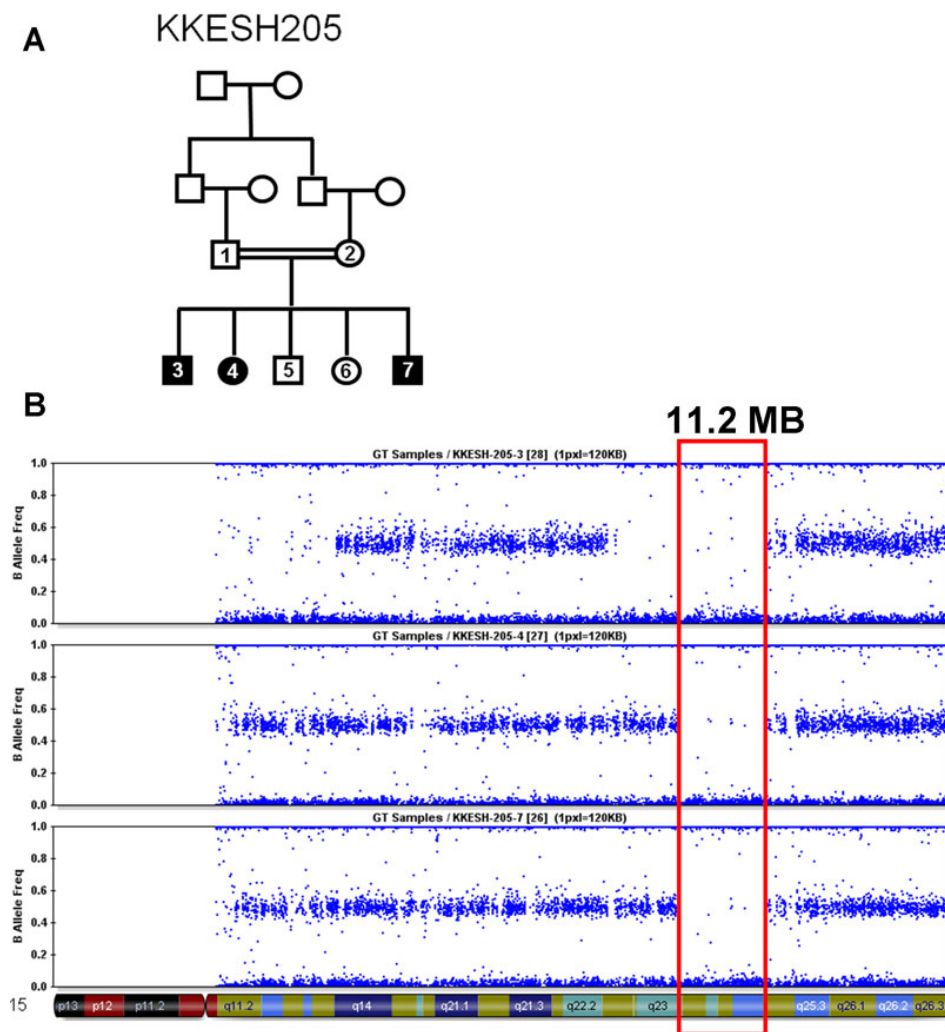


Figure 1. Pedigree and homozygosity mapping of KKESH205. **A:** Pedigree of the KKESH205 family with LCA is shown. Affected, solid symbols; unaffected, open symbols; squares, male; circles, female. **B:** Homozygosity mapping of KKESH205 using high-density SNP arrays. The 11.2 Mb region, which is located on chromosome 15 (red box), is the only homozygous region shared by all three affected members in the whole genome.

further analysis of this candidate mutation was performed. First, this mutation was confirmed with Sanger sequencing (Figure 3B). Second, segregation of this missense mutation in *BBS4* within this LCA family was examined. All members from KKESH205 were genotyped for this mutation with Sanger sequencing; as expected, this allele segregated precisely with the disorder (Figure 3B). Third, to further test if this mutation is indeed rare in the Saudi population, Sanger sequencing was performed on 200 normal matching controls, including 96 from Saudi Arabia. As expected, this mutation was not observed in the control population, indicating that the allele is rare. Furthermore, this mutation is not observed in the [dbSNP130](#) and [1,000 Genomes database](#), indicating that the variant is very rare. This G->C mutation changes an amino acid (Glutamate to Glutamine) that is conserved from lizard to human (Figure 3C). A damage score of 4.91 was assigned to this position based on the [SeattleSNPs](#). Since loss of *BBS4* function is known to cause BBS and *BBS4* knockout mice show severe retinal dystrophy, this novel missense

mutation in *BBS4* is likely to be pathologic in the KKESH205 family [49].

Functional study of the mutant allele: To further test if this missense mutation negatively affects *BBS4* gene function in vivo, we used zebrafish, a model system well established for assessing BBS gene function [42]. Suppression of cilia genes, including *BBS4*, in zebrafish by antisense morpholinos typically produce convergent-extension defects at the 12–14 cell stage, including a shortened body axis, undulating notochord, and broadened somites [44,50-53]. These phenotypes likely reflect abnormal planar cell polarity (PCP) signaling, a hypothesis supported by evidence that BBS proteins genetically and physically interact with components of the PCP pathway [52,54,55]. Researchers have proposed that defects in PCP signaling underlie some clinical features of BBS, including kidney cysts and hearing loss [50,54]. Wild-type embryos (n=280–300) were injected at the 1–2 cell stage with 4.0 ng of a *bbs4* morpholino previously shown to block translation of *bbs4* mRNA [50]. Consistent with previous results, *bbs4* morphants exhibited a shortened body

Percentage

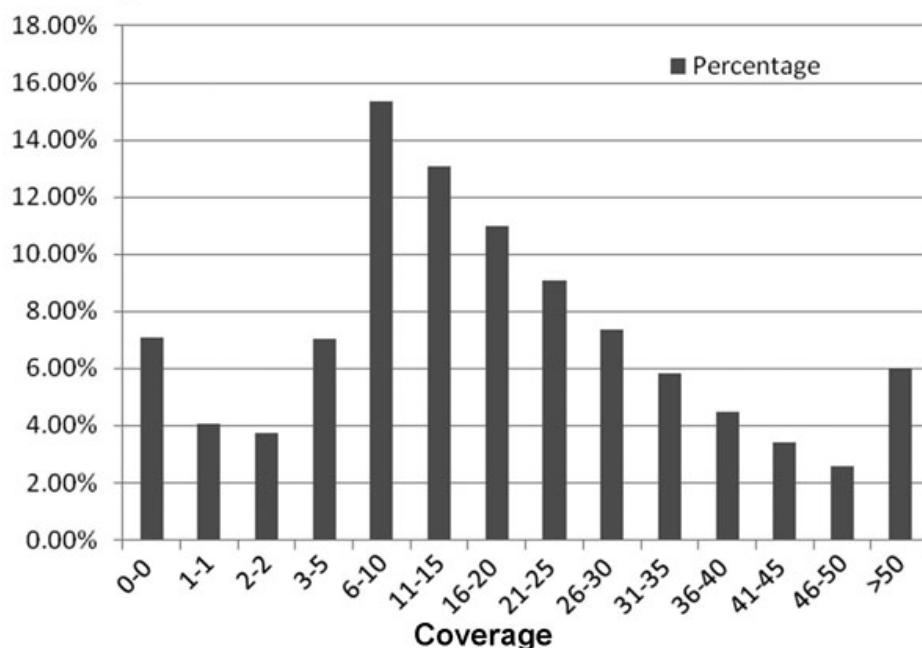


Figure 2. Distribution of sequencing coverage for the targeted region. A total of about 1.6 million reads uniquely map to the exons. Approximately 93% of the coding exons from the targeted region have at least 1X coverage.

axis (Figure 4A, red arrowheads), broadened somites, and a kinked notochord (Figure 4A, red arrow) at the 12–14 somite stage (approximately 15 h post-fertilization). These phenotypes were partially rescued by coinjection of wild-type human *BBS4* mRNA but not the *BBS4* missense allele. Overexpression of either the wild-type or mutant *BBS4* mRNA did not cause any phenotypes. Embryos with normal somites and notochord but a shortened body axis were considered mild, whereas embryos with broad, flattened somites and severely kinked notochords were considered severe. Of the morpholino-injected embryos, 59% had a severe phenotype, and 89% exhibited some defect (Figure 4B). Severe phenotypes were seen in only 27% of the embryos (n=80) when the *bbs4* morpholino was coinjected with 150 pg of wild-type human *BBS4* mRNA and in only 19% of the embryos (n=86) coinjected with 175 pg of wild-type *BBS4* mRNA. These results mirror previous reports of approximately 80% of morphants being rescued by human wild-type *BBS4* mRNA [50]. Importantly, injection of 200 pg of mRNA from the human *BBS4* missense allele did not provide any rescuing effect (n=63). These results indicate that the G253C allele is pathogenic and does not have any readily apparent activity in this assay.

The clinical phenotypes associated with this *BBS4* allele prompted us to investigate whether retinal phenotypes in zebrafish were associated with morpholino suppression of zebrafish *bbs4*. At 5 days post fertilization, zebrafish rod photoreceptors express high levels of rhodopsin that localizes almost exclusively to the photoreceptor outer segments (Figure 4C). To test if *bbs4* is involved in photoreceptors in

zebrafish, retina from 15 embryos from each group as described above were sectioned and stained with rhodopsin. Injection of *bbs4* morpholinos resulted in partial mislocalization of rhodopsin to the inner segment. This result resembles the *Bbs4* knockout mouse [49,56], where photoreceptor outer segments were present but partial rhodopsin mislocalization occurred (Figure 4C, white arrows). When *bbs4* morphants were coinjected with 200 ng of human *BBS4* mRNA, the trafficking defect was reversed, and no rhodopsin mislocalization was observed. In contrast, rhodopsin remained mislocalized in embryos coinjected with morpholino and 200 ng of the *BBS4* missense mRNA.

One possible mechanism by which this missense mutation in *BBS4* could cause a functional defect is to affect protein folding, stability, or localization. To test this possibility, HeLa cells were transfected with wild-type or mutant full-length *BBS4* cDNA in the expression vector pCmv-Tag1 (Stratagene, La Jolla, CA). *BBS4* normally localizes to the pericentriolar region of the cell and functions in recruiting cargo to centriolar satellites [57]. In our study, we found that wild-type endogenous *BBS4* localizes to the pericentriolar region of HeLa cells as described (Figure 5). Similarly, the mutant *BBS4* protein was also expressed and localized to the pericentriolar region of the cell, suggesting that the stable protein was produced and localized normally (Figure 5).

DISCUSSION

Though the eye phenotype of LCA and BBS has some overlap, they are still slightly different. Patients with LCA show

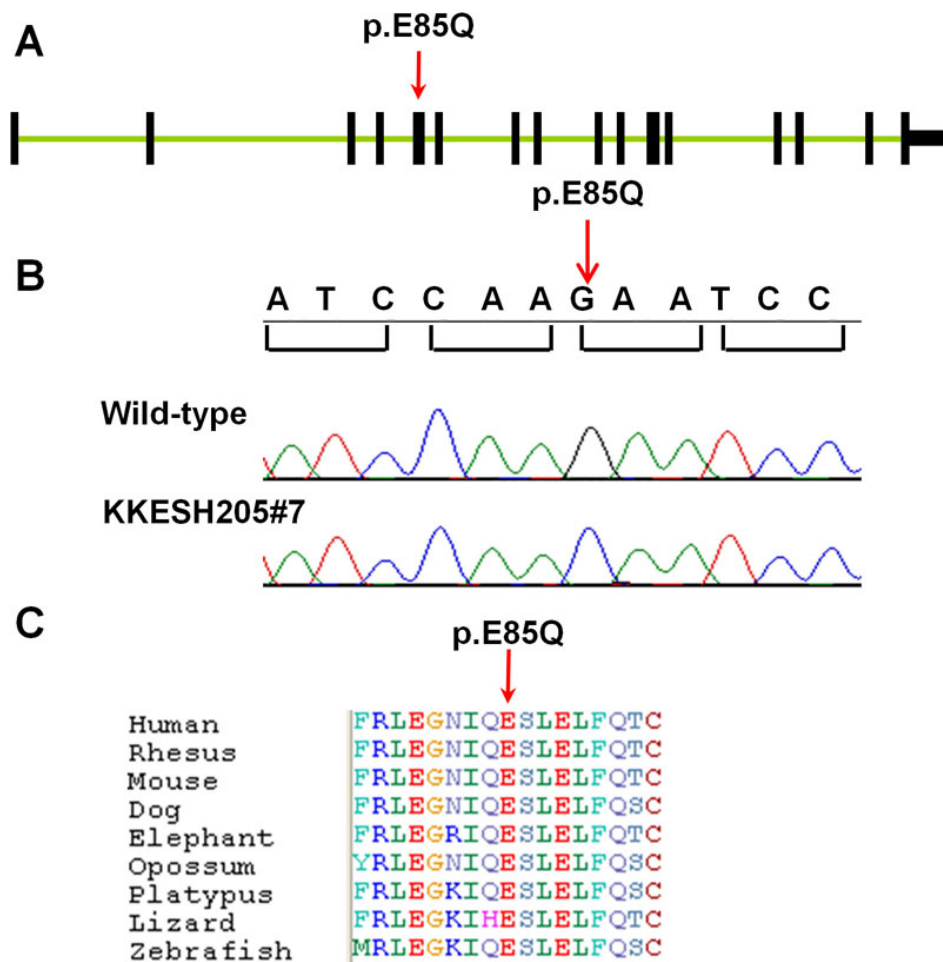


Figure 3. Gene structure of human *BBS4*. **A**: Exon-intron structure of *BBS4*. Exons are indicated as black boxes. The single missense mutation identified is located in the fifth exon (p.E85Q, red arrow). **B**: Sequence traces of wild-type and affected family members. A homozygous mutation from G to C was identified in affected member KKESH205#7 (red arrow). **C**: Amino acid alignment of a portion of the predicted *BBS4* protein from nine different vertebrate species. The mutated amino acid is indicated (p.E85Q, red arrow).

sensory nystagmus, amaurotic pupils, and absent electrical signals on ERG. The BBS eye phenotype is called rod-cone dystrophy, which means visual acuity, dark adaptation, and peripheral visual fields are affected [58]. Patients with BBS have attenuated light- and dark-adapted ERGs [59].

BBS4 comprises 16 exons, and at least 17 mutant alleles have been reported, including nine missense/nonsense changes [60-63], three splicing changes [61] and five in/dels (Figure 3A) [61-63]. *BBS4* is a pericentriolar protein with a key role in recruiting cargo to centriolar satellites and is required for microtubule anchoring and cell cycle progression [57]. The mechanism by which this new allele causes a phenotype resembling LCA without other typical defects associated with BBS is likely due to a partial loss of function that mainly affects the retinal function of *BBS4*. Based on our cell culture assays, this mutation does not affect protein production or localization. Therefore, loss of function is likely due to either a retina-specific reduction of *BBS4* protein levels or a specific functional defect within the retina. The latter case may be more likely since overexpression of the mutant *BBS4* allele does not rescue phenotypes in the zebrafish model. In mice, *BBS4* is known to play an important role in

the proper transport of key phototransduction proteins from photoreceptor inner segments to outer segments [49]. The new allele we report here genetically separates *BBS4* function in the retina versus other tissues, and therefore provides a useful reagent to specifically interrogate *BBS4* function in retinal dystrophy.

In summary, we show that the combination of homozygosity mapping, whole-exome enrichment, and next-generation sequencing provides a sensitive, accurate, and cost-efficient tool for genetic analysis. Large numbers of variants, including rare variants, exist in each individual. As a result, although filtering against dbSNP and 1000 Genomes data can dramatically reduce the number of variants, many remain. Therefore, the main challenge of the whole exome sequencing approach is to devise a strategy to dramatically reduce the number of candidate variants for follow-up studies. One approach is to take advantage of genetic mapping information. In our case, homozygosity mapping narrowed the candidate locus to an 11.2 Mb region. Intersection of candidate variants and the candidate locus resulted in a single remaining variant. In addition, high-throughput functional assays can be used to further test candidate genes. The small

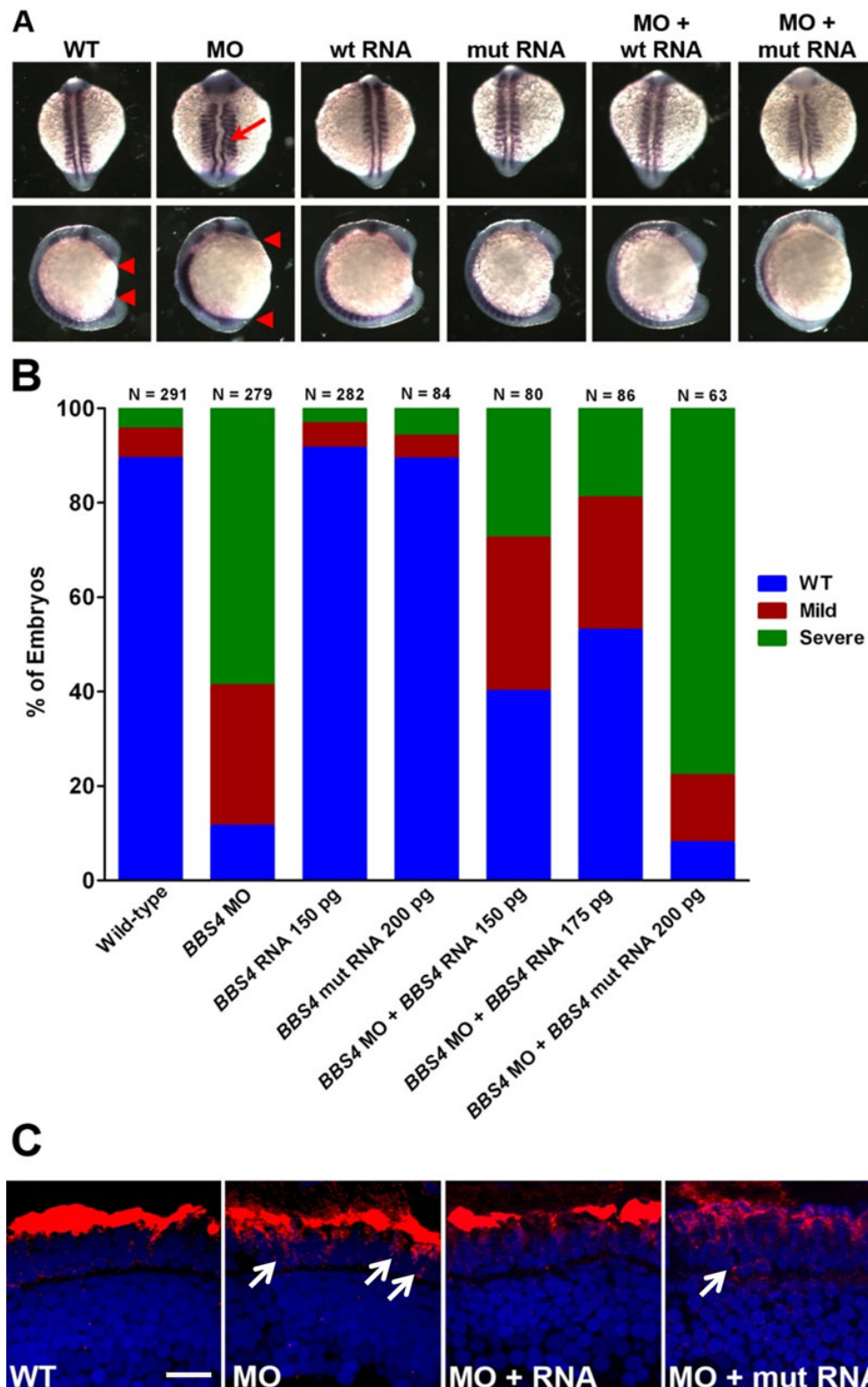
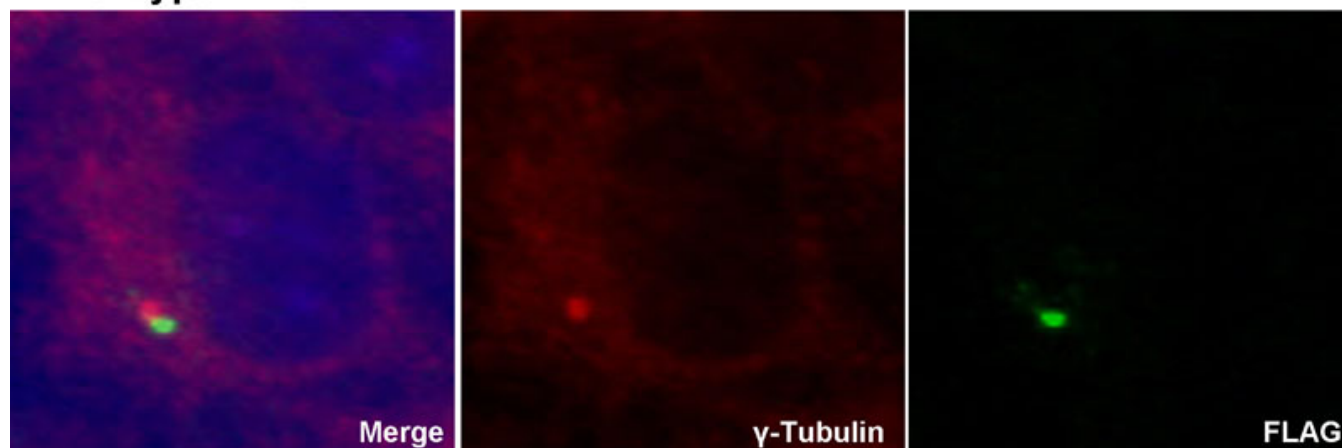


Figure 4. *BBS4* is required for normal zebrafish development and rhodopsin localization. **A**: Representative examples of whole-mounted wild-type (WT) embryos, morpholino-injected (MO) embryos, embryos injected with wild-type (wt) or mutant (mut) human *BBS4* mRNA, or embryos coinjected with morpholino and mRNA. Dorsal view (top row) and lateral view (bottom row) are shown of embryos at the 12–14 somite stage following in situ hybridization with *pax2a* and *myoD* riboprobes. Embryos were categorized phenotypically based on shortened body axis (anterior and posterior ends marked by red triangles) and notochord defects (red arrow). **B**: Quantification of the efficiency of rescue from gastrulation defects following coinjection of *BBS4* morpholino (MO) and mRNA. The number of animals analyzed for each group is noted above each bar. **C**: Retinal cryosections of 5 dpf zebrafish retinas stained for rhodopsin (red). White arrows indicate rhodopsin mislocalization (Scale bar=10 μ m).

Wild Type *BBS4*



Mutant *BBS4*

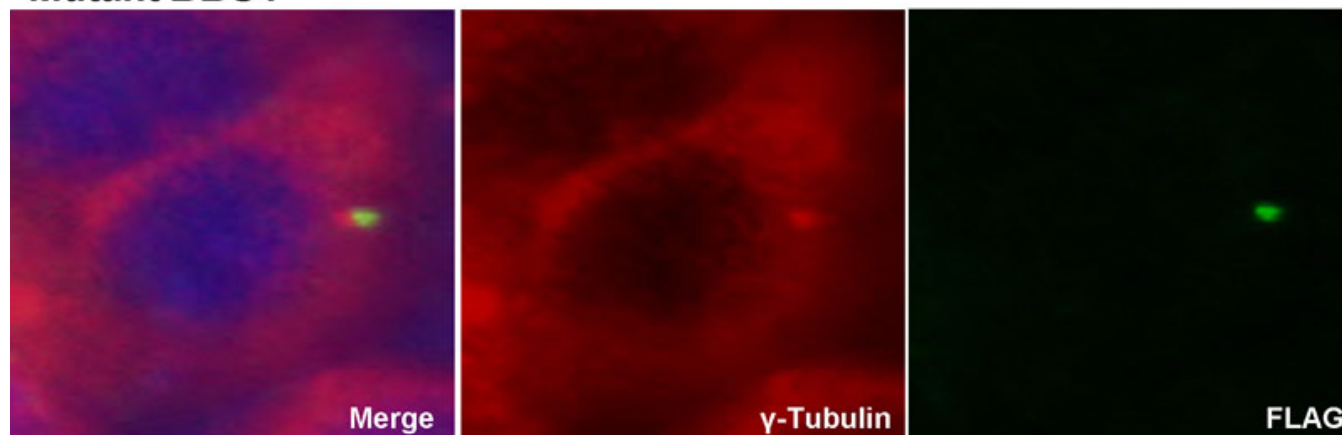


Figure 5. E235Q mutant protein is produced and correctly localizes to the pericentriolar region in HeLa cell culture. Immunofluorescence of FLAG-tagged wild-type and mutant *BBS4* protein in HeLa cells. Cells were stained using an anti-FLAG antibody (green) for *BBS4* expression and anti- γ tubulin antibody (red) for centrosomal localization. Nuclei were stained with DAPI.

size, high fecundity, and experimental tractability of zebrafish make it an excellent system for cost-effective and rapid screening of numerous candidates. Most human genes are conserved in zebrafish, which can therefore serve as a valid model for predicting gene function in humans. The combination of next-generation sequencing, genetic mapping, and high-throughput functional assays will greatly accelerate the identification of human disease genes.

ACKNOWLEDGMENTS

We are indebted to John Cavender, M.D., the Research Director of the King Khalid Eye Specialist Hospital at the time of this study, to the Research Council of KKESH for financial support, and to the staff of the KKESH Research Department for their diligent commitment to this program. In addition, we thank the family reported here for their willing cooperation in this study. We thank Dr. Molly Bray for the SNP genotyping. Dr. Lewis is a Senior Scientific Investigator of Research to Prevent Blindness, New York, NY. This work is supported by grants from the Retina Research Foundation and the National

Eye Institute (R01EY018571 to R.C.). H.W. was supported by postdoctoral fellowship F32EY19430.

REFERENCES

1. Leber T. Uber retinitis pigmentosa und angeborene amaurose. *Albrecht Von Graefes Arch Ophthalmol* 1869; (15):1-25.
2. Dharmaraj SR, Silva ER, Pina AL, Li YY, Yang JM, Carter CR, Loyer MK, El-Hilali HK, Traboulsi EK, Sundin OK, Zhu DK, Koenekoop RK, Maumenee IH. Mutational analysis and clinical correlation in Leber congenital amaurosis. *Ophthalmic Genet* 2000; 21:135-50. [PMID: 11035546]
3. Franceschetti A, Dieterle P. Diagnostic and prognostic importance of the electroretinogram in tapetoretinal degeneration with reduction of the visual field and hemeralopia. *Confin Neurol* 1954; 14:184-6. [PMID: 13190865]
4. den Hollander AI, Koenekoop RK, Yzer S, Lopez I, Arends ML, Voeseke KE, Zonneveld MN, Strom TM, Meitinger T, Brunner HG, Hoyng CB, van den Born LI, Rohrschneider K, Cremers FP. Mutations in the CEP290 (NPHP6) gene are a

- frequent cause of Leber congenital amaurosis. *Am J Hum Genet* 2006; 79:556-61. [PMID: 16909394]
5. den Hollander AI, Koenekoop RK, Mohamed MD, Arts HH, Boldt K, Towns KV, Sedmak T, Beer M, Nagel-Wolfrum K, McKibbin M, Dharmaraj S, Lopez I, Ivings L, Williams GA, Springell K, Woods CG, Jafri H, Rashid Y, Strom TM, van der Zwaag B, Gossens I, Kersten FF, van Wijk E, Veltman JA, Zonneveld MN, van Beersum SE, Maumenee IH, Wolfrum U, Cheetham ME, Ueffing M, Cremers FP, Inglehearn CF, Roepman R. Mutations in LCA5, encoding the ciliary protein lebercilin, cause Leber congenital amaurosis. *Nat Genet* 2007; 39:889-95. [PMID: 17546029]
 6. den Hollander AI, Roepman R, Koenekoop RK, Cremers FP. Leber congenital amaurosis: genes, proteins and disease mechanisms. *Prog Retin Eye Res* 2008; 27:391-419. [PMID: 18632300]
 7. Wang H, den Hollander AI, Moayed Y, Abulimiti A, Li Y, Collin RW, Hoyng CB, Lopez I, Abboud EB, Al-Rajhi AA, Bray M, Lewis RA, Lupski JR, Mardon G, Koenekoop RK, Chen R. Mutations in SPATA7 cause Leber congenital amaurosis and juvenile retinitis pigmentosa. *Am J Hum Genet* 2009; 84:380-7. [PMID: 19268277]
 8. Cremers FP, van den Hurk JA, den Hollander AI. Molecular genetics of Leber congenital amaurosis. *Hum Mol Genet* 2002; 11:1169-76. [PMID: 12015276]
 9. Janecke AR, Thompson DA, Utermann G, Becker C, Hübner CA, Schmid E, McHenry CL, Nair AR, Rüschemdorf F, Heckenlively J, Wissinger B, Nürnberg P, Gal A. Mutations in RDH12 encoding a photoreceptor cell retinol dehydrogenase cause childhood-onset severe retinal dystrophy. *Nat Genet* 2004; 36:850-4. [PMID: 15258582]
 10. Perrault I, Hanein S, Gerber S, Barbet F, Ducroq D, Dollfus H, Hamel C, Dufier JL, Munnich A, Kaplan J, Rozet JM. Retinal dehydrogenase 12 (RDH12) mutations in leber congenital amaurosis. *Am J Hum Genet* 2004; 75:639-46. [PMID: 15322982]
 11. Thompson DA, Li Y, McHenry CL, Carlson TJ, Ding X, Sieving PA, Apfelstedt-Sylla E, Gal A. Mutations in the gene encoding lecithin retinol acyltransferase are associated with early-onset severe retinal dystrophy. *Nat Genet* 2001; 28:123-4. [PMID: 11381255]
 12. Pang J, Boye SE, Lei B, Boye SL, Everhart D, Ryals R, Umiono Y, Rohrer B, Alexander J, Li J, Dai X, Li Q, Chang B, Barlow R, Hauswirth WW. Self-complementary AAV-mediated gene therapy restores cone function and prevents cone degeneration in two models of Rpe65 deficiency. *Gene Ther* 2010; 17:815-26. [PMID: 20237510]
 13. Maguire AM, Simonelli F, Pierce EA, Pugh EN Jr, Mingozzi F, Bennicelli J, Banfi S, Marshall KA, Testa F, Surace EM, Rossi S, Lyubarsky A, Arruda VR, Konkle B, Stone E, Sun J, Jacobs J, Dell'Osso L, Hertle R, Ma JX, Redmond TM, Zhu X, Hauck B, Zelenia O, Shindler KS, Maguire MG, Wright JF, Volpe NJ, McDonnell JW, Auricchio A, High KA, Bennett J. Safety and Efficacy of Gene Transfer for Leber's Congenital Amaurosis. *N Engl J Med* 2008; 358:2240-8. [PMID: 18441370]
 14. Sundaresan P, Vijayalakshmi P, Thompson S, Ko AC, Fingert JH, Stone EM. Mutations that are a common cause of Leber congenital amaurosis in northern America are rare in southern India. *Mol Vis* 2009; 15:1781-7. [PMID: 19753312]
 15. Perrault I, Delphin N, Hanein S, Gerber S, Dufier JL, Roche O, Defoort-Dhellemmes S, Dollfus H, Fazzi E, Munnich A, Kaplan J, Rozet JM. Spectrum of NPHP6/CEP290 mutations in Leber congenital amaurosis and delineation of the associated phenotype. *Hum Mutat* 2007; 28:416. [PMID: 17345604]
 16. Simonelli F, Ziviello C, Testa F, Rossi S, Fazzi E, Bianchi PE, Fossarello M, Signorini S, Bertone C, Galantuomo S, Brancati F, Valente EM, Ciccociola A, Rinaldi E, Auricchio A, Banfi S. Clinical and molecular genetics of Leber's congenital amaurosis: a multicenter study of Italian patients. *Invest Ophthalmol Vis Sci* 2007; 48:4284-90. [PMID: 17724218]
 17. Vallespin E, Lopez-Martinez MA, Cantalapiedra D, Riveiro-Alvarez R, Aguirre-Lamban J, Avila-Fernandez A, Villaverde C, Trujillo-Tiebas MJ, Ayuso C. Frequency of CEP290 c.2991_1655A>G mutation in 175 Spanish families affected with Leber congenital amaurosis and early-onset retinitis pigmentosa. *Mol Vis* 2007; 13:2160-2. [PMID: 18079693]
 18. Baala L, Audollent S, Martinovic J, Ozilou C, Babron MC, Sivanandamoorthy S, Saunier S, Salomon R, Gonzales M, Rattenberry E, Esculpavit C, Toutain A, Moraine C, Parent P, Marcocelles P, Dauge MC, Roume J, Le Merrer M, Meiner V, Meir K, Menez F, Beaufrère AM, Francannet C, Tantau J, Sinico M, Dumez Y, MacDonald F, Munnich A, Lyonnet S, Gubler MC, Génin E, Johnson CA, Vekemans M, Encha-Razavi F, Attié-Bitach T. Pleiotropic effects of CEP290 (NPHP6) mutations extend to Meckel syndrome. *Am J Hum Genet* 2007; 81:170-9. [PMID: 17564974]
 19. Frank V, den Hollander AI, Bruchle NO, Zonneveld MN, Nürnberg G, Becker C, Du Bois G, Kendziorra H, Roosing S, Senderek J, Nürnberg P, Cremers FP, Zerres K, Bergmann C. Mutations of the CEP290 gene encoding a centrosomal protein cause Meckel-Gruber syndrome. *Hum Mutat* 2008; 29:45-52. [PMID: 17705300]
 20. Helou J, Otto EA, Attanasio M, Allen SJ, Parisi MA, Glass I, Utsch B, Hashmi S, Fazzi E, Omran H, O'Toole JF, Sayer JA, Hildebrandt F. Mutation analysis of NPHP6/CEP290 in patients with Joubert syndrome and Senior-Loken syndrome. *J Med Genet* 2007; 44:657-63. [PMID: 17617513]
 21. Leitch CC, Zaghoul NA, Davis EE, Stoetzel C, Diaz-Font A, Rix S, Alfadhel M, Lewis RA, Eyaid W, Banin E, Dollfus H, Beales PL, Badano JL, Katsanis N. Hypomorphic mutations in syndromic encephalocele genes are associated with Bardet-Biedl syndrome. *Nat Genet* 2008; 40:443-8. [PMID: 18327255]
 22. Sayer JA, Otto EA, O'Toole JF, Nürnberg G, Kennedy MA, Becker C, Hennies HC, Helou J, Attanasio M, Fausett BV, Utsch B, Khanna H, Liu Y, Drummond I, Kawakami I, Kusakabe T, Tsuda M, Ma L, Lee H, Larson RG, Allen SJ, Wilkinson CJ, Nigg EA, Shou C, Lillo C, Williams DS, Hoppe B, Kemper MJ, Neuhaus T, Parisi MA, Glass IA, Petry M, Kispert A, Gloy J, Ganner A, Walz G, Zhu X, Goldman D, Nürnberg P, Swaroop A, Leroux MR, Hildebrandt F. The centrosomal protein nephrocystin-6 is mutated in Joubert syndrome and activates transcription factor ATF4. *Nat Genet* 2006; 38:674-81. [PMID: 16682973]
 23. Valente EM, Silhavy JL, Brancati F, Barrano G, Krishnaswami SR, Castori M, Lancaster MA, Boltshausen E, Boccone L, Al-Gazali L, Fazzi E, Signorini S, Louie CM, Bellacchio E,

- International Joubert Syndrome Related Disorders Study Group. Bertini E, Dallapiccola B, Gleeson JG. Mutations in CEP290, which encodes a centrosomal protein, cause pleiotropic forms of Joubert syndrome. *Nat Genet* 2006; 38:623-5. [PMID: 16682970]
24. Riazuddin SA, Iqbal M, Wang Y, Masuda T, Chen Y, Bowne S, Sullivan LS, Waseem NH, Bhattacharya S, Daiger SP, Zhang K, Khan SN, Riazuddin S, Hejtmancik JF, Sieving PA, Zack DJ, Katsanis N. A splice-site mutation in a retina-specific exon of BBS8 causes nonsyndromic retinitis pigmentosa. *Am J Hum Genet* 2010; 86:805-12. [PMID: 20451172]
 25. Ansorge WJ. Next-generation DNA sequencing techniques. *New Biotechnol* 2009; 25:195-203. [PMID: 19429539]
 26. Mardis ER. The impact of next-generation sequencing technology on genetics. *Trends Genet* 2008; 24:133-41. [PMID: 18262675]
 27. Mardis ER. Next-generation DNA sequencing methods. *Annu Rev Genomics Hum Genet* 2008; 9:387-402. [PMID: 18576944]
 28. Shendure J, Ji H. Next-generation DNA sequencing. *Nat Biotechnol* 2008; 26:1135-45. [PMID: 18846087]
 29. Hodges E, Rooks M, Xuan Z, Bhattacharjee A, Benjamin Gordon D, Brizuela L, Richard McCombie W, Hannon GJ. Hybrid selection of discrete genomic intervals on custom-designed microarrays for massively parallel sequencing. *Nat Protoc* 2009; 4:960-74. [PMID: 19478811]
 30. Li Y, Vinckenbosch N, Tian G, Huerta-Sanchez E, Jiang T, Jiang H, Albrechtsen A, Andersen G, Cao H, Korneliusen T, Grarup N, Guo Y, Hellman I, Jin X, Li Q, Liu J, Liu X, Sparsø T, Tang M, Wu H, Wu R, Yu C, Zheng H, Astrup A, Bolund L, Holmkvist J, Jørgensen T, Kristiansen K, Schmitz O, Schwartz TW, Zhang X, Li R, Yang H, Wang J, Hansen T, Pedersen O, Nielsen R, Wang J. Resequencing of 200 human exomes identifies an excess of low-frequency non-synonymous coding variants. *Nat Genet* 2010; 42:969-72. [PMID: 20890277]
 31. Kim DW, Nam SH, Kim RN, Choi SH, Park HS. Whole human exome capture for high-throughput sequencing. *Genome* 2010; 53:568-74. [PMID: 20616878]
 32. Teer JK, Mullikin JC. Exome sequencing: the sweet spot before whole genomes. *Hum Mol Genet* 2010; 19:R145-51. [PMID: 20705737]
 33. Rehman AU, Morell RJ, Belyantseva IA, Khan SY, Boger ET, Shahzad M, Ahmed ZM, Riazuddin S, Khan SN, Riazuddin S, Friedman TB. Targeted capture and next-generation sequencing identifies C9orf75, encoding taperin, as the mutated gene in nonsyndromic deafness DFNB79. *Am J Hum Genet* 2010; 86:378-88. [PMID: 20170899]
 34. Volpi L, Roversi G, Colombo EA, Leijsten N, Concolino D, Calabria A, Mencarelli MA, Fimiani M, Macciardi F, Pfundt R, Schoenmakers EF, Larizza L. Targeted next-generation sequencing appoints c16orf57 as clericuzio-type poikiloderma with neutropenia gene. *Am J Hum Genet* 2010; 86:72-6. [PMID: 20004881]
 35. Choi M, Scholl UI, Ji W, Liu T, Tikhonova IR, Zumbo P, Nayir A, Bakkaloğlu A, Ozen S, Sanjad S, Nelson-Williams C, Farhi A, Mane S, Lifton RP. Genetic diagnosis by whole exome capture and massively parallel DNA sequencing. *Proc Natl Acad Sci USA* 2009; 106:19096-101. [PMID: 19861545]
 36. Ng SB, Buckingham KJ, Lee C, Bigham AW, Tabor HK, Dent KM, Huff CD, Shannon PT, Jabs EW, Nickerson DA, Shendure J, Bamshad MJ. Exome sequencing identifies the cause of a mendelian disorder. *Nat Genet* 2010; 42:30-5. [PMID: 19915526]
 37. Ng SB, Bigham AW, Buckingham KJ, Hannibal MC, McMillin MJ, Gildersleeve HI, Beck AE, Tabor HK, Cooper GM, Mefford HC, Lee C, Turner EH, Smith JD, Rieder MJ, Yoshiura K, Matsumoto N, Ohta T, Niikawa N, Nickerson DA, Bamshad MJ, Shendure J. Exome sequencing identifies MLL2 mutations as a cause of Kabuki syndrome. *Nat Genet* 2010; 42:790-3. [PMID: 20711175]
 38. Bilgüvar K, Oztürk AK, Louvi A, Kwan KY, Choi M, Tatli B, Yalnizoğlu D, Tüysüz B, Çağlayan AO, Gökben S, Kaymakçalan H, Barak T, Bakircioğlu M, Yasuno K, Ho W, Sanders S, Zhu Y, Yilmaz S, Dinçer A, Johnson MH, Bronen RA, Koçer N, Per H, Mane S, Pamir MN, Yalçinkaya C, Kumandaş S, Topçu M, Özmen M, Sestan N, Lifton RP, State MW, Günel M. Whole-exome sequencing identifies recessive WDR62 mutations in severe brain malformations. *Nature* 2010; 467:207-10. [PMID: 20729831]
 39. Haack TB, Danhauser K, Haberberger B, Hoser J, Strecker V, Boehm D, Uziel G, Lamantea E, Invernizzi F, Poulton J, Rolinski B, Iuso A, Biskup S, Schmidt T, Mewes HW, Wittig I, Meitinger T, Zeviani M, Prokisch H. Exome sequencing identifies ACAD9 mutations as a cause of complex I deficiency. *Nat Genet* 2010; 42:1131-4. [PMID: 21057504]
 40. Bonnefond A, Durand E, Sand O, De Graeve F, Gallina S, Busiah K, Lobbens S, Simon A, Bellanné-Chantelot C, Létourneau L, Scharfmann R, Delplanque J, Sladek R, Polak M, Vaxillaire M, Froguel P. Molecular diagnosis of neonatal diabetes mellitus using next-generation sequencing of the whole exome. *PLoS ONE* 2010; 5:e13630. [PMID: 21049026]
 41. Walsh T, Shahin H, Elkan-Miller T, Lee MK, Thornton AM, Roeb W, Abu Rayyan A, Loulus S, Avraham KB, King MC, Kanaan M. Whole exome sequencing and homozygosity mapping identify mutation in the cell polarity protein GSPM2 as the cause of nonsyndromic hearing loss DFNB82. *Am J Hum Genet* 2010; 87:90-4. [PMID: 20602914]
 42. Zaghoul NA, Katsanis N. Mechanistic insights into Bardet-Biedl syndrome, a model ciliopathy. *J Clin Invest* 2009; 119:428-37. [PMID: 19252258]
 43. Akimenko MA, Johnson SL, Westerfield M, Ekker M. Differential induction of four msx homeobox genes during fin development and regeneration in zebrafish. *Development* 1995; 121:347-57. [PMID: 7768177]
 44. Khanna H, Davis EE, Murga-Zamalloa CA, Estrada-Cuzcano A, Lopez I, den Hollander AI, Zonneveld MN, Othman MI, Waseem N, Chakarova CF, Maubaret C, Diaz-Font A, MacDonald I, Muzny DM, Wheeler DA, Morgan M, Lewis LR, Logan CV, Tan PL, Beer MA, Inglehearn CF, Lewis RA, Jacobson SG, Bergmann C, Beales PL, Attié-Bitach T, Johnson CA, Otto EA, Bhattacharya SS, Hildebrandt F, Gibbs RA, Koeneke RK, Swaroop A, Katsanis N. A common allele in RPGRIP1L is a modifier of retinal degeneration in ciliopathies. *Nat Genet* 2009; 41:739-45. [PMID: 19430481]

45. Jowett T, Lettice L. Whole-mount in situ hybridizations on zebrafish embryos using a mixture of digoxigenin- and fluorescein-labelled probes. *Trends Genet* 1994; 10:73-4. [PMID: 8178366]
46. Li H, Durbin R. Fast and accurate short read alignment with Burrows-Wheeler transform. *Bioinformatics* 2009; 25:1754-60. [PMID: 19451168]
47. Li H, Handsaker B, Wysoker A, Fennell T, Ruan J, Homer N, Marth G, Abecasis G, Durbin R. 1000 Genome Project Data Processing Subgroup. The Sequence Alignment/Map format and SAMtools. *Bioinformatics* 2009; 25:2078-9. [PMID: 19505943]
48. Tobin JL, Beales PL. Bardet-Biedl syndrome: beyond the cilium. *Pediatr Nephrol* 2007; 22:926-36. [PMID: 17357787]
49. LiHHandsakerBWysockerAFennellTRuanJHomerNMMarthGAbecasisGDurbinR1000 Genome Project Data Processing Subgroup. Impaired photoreceptor protein transport and synaptic transmission in a mouse model of Bardet-Biedl syndrome. *Vision Res* 2007; 47:3394-407. http://www.ncbi.nlm.nih.gov/entrez/query.fcgi?cmd=Retrieve&db=PubMed&list_uids=18022666&dopt=Abstract [PubMed: 18022666]
50. Zaghoul NA, Liu Y, Gerdes JM, Gascue C, Oh EC, Leitch CC, Bromberg Y, Binkley J, Leibel RL, Sidow A, Badano JL, Katsanis N. Functional analyses of variants reveal a significant role for dominant negative and common alleles in oligogenic Bardet-Biedl syndrome. *Proc Natl Acad Sci USA* 2010; 107:10602-7. [PMID: 20498079]
51. Badano JL, Leitch CC, Ansley SJ, May-Simera H, Lawson S, Lewis RA, Beales PL, Dietz HC, Fisher S, Katsanis N. Dissection of epistasis in oligogenic Bardet-Biedl syndrome. *Nature* 2006; 439:326-30. [PMID: 16327777]
52. Gerdes JM, Liu Y, Zaghoul NA, Leitch CC, Lawson SS, Kato M, Beachy PA, Beales PL, DeMartino GN, Fisher S, Badano JL, Katsanis N. Disruption of the basal body compromises proteasomal function and perturbs intracellular Wnt response. *Nat Genet* 2007; 39:1350-60. [PMID: 17906624]
53. Stoetzel C, Laurier V, Davis EE, Muller J, Rix S, Badano JL, Leitch CC, Salem N, Chouery E, Corbani S, Jalk N, Vicaire S, Sarda P, Hamel C, Lacombe D, Holder M, Odent S, Holder S, Brooks AS, Elcioglu NH, Silva ED, Rossillion B, Sigaudy S, de Ravel TJ, Lewis RA, Leheup B, Verloes A, Amati-Bonneau P, Mégarbané A, Poch O, Bonneau D, Beales PL, Mandel JL, Katsanis N, Dollfus H. BBS10 encodes a vertebrate-specific chaperonin-like protein and is a major BBS locus. *Nat Genet* 2006; 38:521-4. [PMID: 16582908]
54. Ross AJ, May-Simera H, Eichers ER, Kai M, Hill J, Jagger DJ, Leitch CC, Chapple JP, Munro PM, Fisher S, Tan PL, Phillips HM, Leroux MR, Henderson DJ, Murdoch JN, Copp AJ, Eliot MM, Lupski JR, Kemp DT, Dollfus H, Tada M, Katsanis N, Forge A, Beales PL. Disruption of Bardet-Biedl syndrome ciliary proteins perturbs planar cell polarity in vertebrates. *Nat Genet* 2005; 37:1135-40. [PMID: 16170314]
55. May-Simera HL, Kai M, Hernandez V, Osborn DP, Tada M, Beales PL. Bbs8, together with the planar cell polarity protein Vangl2, is required to establish left-right asymmetry in zebrafish. *Dev Biol* 2010; 345:215-25. [PMID: 20643117]
56. Mykytyn K, Mullins RF, Andrews M, Chiang AP, Swiderski RE, Yang B, Braun T, Casavant T, Stone EM, Sheffield VC. Bardet-Biedl syndrome type 4 (BBS4)-null mice implicate Bbs4 in flagella formation but not global cilia assembly. *Proc Natl Acad Sci USA* 2004; 101:8664-9. [PMID: 15173597]
57. Kim JC, Badano JL, Sibold S, Esmail MA, Hill J, Hoskins BE, Leitch CC, Venner K, Ansley SJ, Ross AJ, Leroux MR, Katsanis N, Beales PL. The Bardet-Biedl protein BBS4 targets cargo to the pericentriolar region and is required for microtubule anchoring and cell cycle progression. *Nat Genet* 2004; 36:462-70. [PMID: 15107855]
58. Waters AM, Beales PL. Bardet-Biedl Syndrome. University of Washington, Seattle, 1993
59. Cannon PS, Clayton-Smith J, Beales PL, Lloyd IC. Bardet-biedl syndrome: an atypical phenotype in brothers with a proven BBS1 mutation. *Ophthalmic Genet* 2008; 29:128-32. [PMID: 18766993]
60. Katsanis N, Eichers ER, Ansley SJ, Lewis RA, Kayserili H, Hoskins BE, Scambler PJ, Beales PL, Lupski JR. BBS4 is a minor contributor to Bardet-Biedl syndrome and may also participate in triallelic inheritance. *Am J Hum Genet* 2002; 71:22-9. [PMID: 12016587]
61. Mykytyn K, Braun T, Carmi R, Haider NB, Searby CC, Shastri M, Beck G, Wright AF, Iannaccone A, Elbedour K, Riise R, Baldi A, Raas-Rothschild A, Gorman SW, Duhl DM, Jacobson SG, Casavant T, Stone EM, Sheffield VC. Identification of the gene that, when mutated, causes the human obesity syndrome BBS4. *Nat Genet* 2001; 28:188-91. [PMID: 11381270]
62. Karmous-Benailly H, Martinovic J, Gubler MC, Sirot Y, Clech L, Ozilou C, Auge J, Brahimi N, Etchevers H, Deraut E, Esculpavit C, Audollent S, Goudefroye G, Gonzales M, Tantau J, Loget P, Joubert M, Gaillard D, Jeanne-Pasquier C, Delezoide AL, Peter MO, Plessis G, Simon-Bouy B, Dollfus H, Le Merrer M, Munnich A, Encha-Razavi F, Vekemans M, Attié-Bitach T. Antenatal presentation of Bardet-Biedl syndrome may mimic Meckel syndrome. *Am J Hum Genet* 2005; 76:493-504. [PMID: 15666242]
63. Hoskins BE, Thorn A, Scambler PJ, Beales PL. Evaluation of multiplex capillary heteroduplex analysis: a rapid and sensitive mutation screening technique. *Hum Mutat* 2003; 22:151-7. [PMID: 12872256]

Appendix 1.

To access the data, click or select the words “[Appendix 1.](#)” This will initiate the download of a compressed (pdf) archive that contains the file.